

**PHOTODEGRADATION PERFORMANCES OF
LOW-DENSITY POLYETHYLENE COMPOSITES
LOADED WITH PHOTOCATALYSTS**

NELVI SUTANTO

UNIVERSITI SAINS MALAYSIA

2019

**PHOTODEGRADATION PERFORMANCES OF
LOW-DENSITY POLYETHYLENE COMPOSITES
LOADED WITH PHOTOCATALYSTS**

by

NELVI SUTANTO

**Thesis submitted in fulfilment of the requirements
for the degree of
Doctor of Philosophy**

OCTOBER 2019

ACKNOWLEDGEMENT

My deepest appreciation goes to my main supervisor Prof. Ir. Dr. Srimala Sreekantan who has patiently assisted me in successfully complete this research work as well as writing a high standard PhD thesis at Universiti Sains Malaysia. Thanks also go to my co-supervisors; Assoc. Prof. Dr. Pung Swee Yong and Prof. Hazizan Md Akil for their guidance, invaluable suggestions and encouragement. Thankful also goes to Transdisciplinary Research Grant Scheme (TRGS) grant (grant no. 6769002).

Finally, thanks to all academic, administrative and technical staffs from School of Materials and Mineral Resources Engineering (SMMRE) for their support and help to finish my research work. Special thanks to friends and family for helping through the journey.

TABLE OF CONTENTS

ACKNOWLEDGEMENT	ii
TABLE OF CONTENTS.....	iii
LIST OF TABLES	viii
LIST OF FIGURES	x
LIST OF SYMBOLS	xvii
LIST OF ABBREVIATIONS	xviii
ABSTRAK	xix
ABSTRACT	xxi
CHAPTER 1 INTRODUCTION	1
1.1 Research Background.....	1
1.2 Problem Statement	4
1.3 Research Objectives	6
1.4 Research Scope	6
1.5 Thesis Outline	8
CHAPTER 2 LITERATURE REVIEW	10
2.1 Polymer Waste Generation.....	10
2.2 Current Waste Management Technologies	11
2.2.1 Landfill	12
2.2.2 Incineration.....	12
2.2.3 Recycling.....	13
2.3 Several Other Degradation Methods on PE	14
2.3.1 Thermal Degradation.....	14
2.3.2 Biodegradation	17
2.3.3 Photodegradation.....	18

2.3.3(a)	Mechanism I (Chain Initiation).....	19
2.3.3(b)	Mechanism II (Chain Propagation).....	21
2.3.3(c)	Mechanism III (Chain Termination).....	23
2.4	Factor Affecting the Photocatalyst and Polymer Degradation.....	23
2.4.1	Choice of Photocatalyst.....	23
2.4.1(a)	Photocatalyst to Degrade Organic Pollutant.....	24
2.4.1(b)	Photocatalyst to Degrade Polymer.....	30
2.4.2	Polymer Matrix	33
2.4.2(a)	Water Absorption.....	33
2.4.2(b)	Degree of Crystallinity.....	35
2.4.2(c)	Functional Group and Chemical Composition	36
2.4.2(d)	Hydrophobic Characteristic	37
2.4.2(e)	Molecular Weight	38
2.4.3	Environmental Conditions.....	39
2.4.3(a)	Humidity	39
2.4.3(b)	Temperature	40
2.4.3(c)	Light penetration and type of light	40
CHAPTER 3	METHODOLOGY	42
3.1	Introduction	42
3.2	Raw Materials	42
3.3	Experimental Procedure	44
3.3.1	Synthesis of Photocatalyst.....	46
3.3.1(a)	Synthesis of ZnO	46
3.3.1(b)	Synthesis of TiO ₂	47
3.3.1(c)	Synthesis of Coupled Oxide ZnO/TiO ₂	47
3.3.1(d)	Synthesis of g-C ₃ N ₄ /3ZT	50
3.3.2	Fabrication of Pure LDPE and LDPE Composite Films.....	50
3.3.2(a)	Fabrication of LDPE films with 1 mm thickness by compression molding method.....	50
3.3.2(b)	Fabrication of LDPE films with 0.1 mm and 0.035 mm thickness by wet casting method	52
3.3.3	Fabrication of LDPE composite with PVA functionalized photocatalyst.....	53

3.4	Characterization Techniques	54
3.4.1	X-ray Diffraction (XRD).....	55
3.4.2	Field Emission Scanning Electron Microscope (FESEM)	56
3.4.3	High Resolution Transmission Electron Microscope (HRTEM) ...	57
3.4.4	Energy Dispersive X-ray spectroscopy (EDX)	57
3.4.5	UV Vis Spectroscopy Diffuse Reflectance Spectroscopy (UV Vis DRS).....	58
3.4.6	Tensile Testing	59
3.4.7	Fourier Transform Infrared Spectroscopy (FTIR)	60
3.4.8	Differential Scanning Calorimetry (DSC) Testing.....	61
3.4.9	Evaluation of Photocatalytic Activity for photocatalyst	61
3.4.10	OH• Scavenger Test for optimized photocatalyst sample.....	62
3.4.11	Reactive oxygen species (ROS) for polymer composite films.....	62
3.4.12	Degradation rate of Films.....	63
3.4.13	Weight Loss Analysis.....	63
3.4.14	Water Absorption for LDPE composite films.....	64
CHAPTER 4	RESULTS AND DISCUSSION	65
4.1	Effect of ratio of ZnO/TiO ₂ and Photocatalytic Activity of Methylene Blue	65
4.1.1	Structural Property	65
4.1.2	Morphology	68
4.1.3	Bandgap Evaluation	70
4.1.4	Photocatalytic Degradation of Methylene Blue	72
4.1.5	High Resolution Transmission Electron Microscopy (HRTEM)...	75
4.2	Effect of g-C ₃ N ₄ content in 3ZnO/-c-Zn ₂ Ti ₃ O ₈ and Photocatalytic Activity of Methylene Blue.....	77
4.2.1	Crystal Structure of 3ZT Loaded with g-C ₃ N ₄	77
4.2.2	Bandgap Evaluation of 3ZT Loaded with g-C ₃ N ₄	79

4.2.3	Photodegradation of MB Dye Solution	81
4.2.4	HRTEM of 10C-3ZT	86
4.2.5	Analysis of hydroxyl radical (\bullet OH)	89
4.3	Structural, Tensile and Degradation of LDPE Composites with 1.0 mm thickness prepared by compression molding method.....	91
4.3.1	Appearance of 10C-3ZT LDPE composites.....	91
4.3.2	Structural Property	92
4.3.3	Differential Scanning Calorimetry (DSC).....	94
4.3.4	Morphology	94
4.3.5	Fourier Transform Infrared Spectroscopy (FTIR)	96
4.3.6	Tensile Properties	99
4.3.7	Carbonyl Index	101
4.3.8	Photodegradation.....	102
4.4	Structural, Tensile and Degradation of LDPE Composites with 0.1 mm and 0.035 mm thickness prepared by wet casting method	103
4.4.1	Appearance of LDPE composites	103
4.4.2	Structural Property of the LDPE composite.....	106
4.4.3	Differential Scanning Calorimetry (DSC).....	109
4.4.4	Morphology	110
4.4.5	Fourier Transform Infrared Spectroscopy (FTIR)	116
4.4.6	Tensile Properties	122
4.4.7	Carbonyl Index	124
4.4.8	Photodegradation.....	126
4.4.9	Photocatalytic activity and Scavenger Test.....	127
4.4.10	Photodegradation Mechanism	132
4.5	The effect of PVA functionalized photocatalyst in LDPE composite films	134
4.5.1	Appearance of PVA functionalized photocatalyst in LDPE composite films	135

4.5.2	Morphology	136
4.5.3	Water Absorption	138
4.5.4	Fourier Transform Infrared Spectroscopy (FTIR)	140
4.5.5	Photocatalytic activity and Scavenger Test.....	144
4.5.6	Weight loss and carbonyl index	145
CHAPTER 5 CONCLUSIONS AND FUTURE RECOMMENDATIONS.....		147
5.1	Conclusions	147
5.2	Recommendations for Future Researches	148
REFERENCES.....		149
APPENDIX A: MOL RATIO CALCULATION		
APPENDIX B: XRD of POLYETHYLENE		
APPENDIX C: DEGRADATION RATE CALCULATION		
APPENDIX D: CARBONYL INDEX CALCULATION		
APPENDIX E: IR ABSORPTION RANGE		
LIST OF PUBLICATIONS		

LIST OF TABLES

Table 2.1	Summaries of polyethylene degradation methods	16
Table 2.2	Summaries of photocatalyst and degradation rate of dye contaminants	27
Table 2.3	The effect of photocatalyst on the degradation rate of polymer	31
Table 2.4	Water absorption of polymer	34
Table 2.5	The effect of photocatalyst on polymer's degree of crystallinity	36
Table 2.6	The effect of molecular weight on polymer's weight loss	38
Table 2.7	Summary of wavelength of light and energy contained at this wavelength	41
Table 2.8	Summary of type of bond and energy to break the bond in PE (Martínez-Romo et al., 2015; Sackey et al., 2015)	41
Table 3.1	Raw materials and chemicals used in preparing photocatalyst and PC loaded LDPE composite films.....	43
Table 3.2	Mol ratio and amount of solvent used in synthesis of ZnO/TiO ₂	49
Table 3.3	Constant parameter for ZnO/TiO ₂ synthesis process	49
Table 3.4	Details of g-C ₃ N ₄ concentrations	50
Table 3.5	Constant parameters of Haake internal mixing process.....	51
Table 3.6	Constant parameters of Compression moulding process	51
Table 3.7	Variation of 10C-3ZT photocatalyst concentration in 1 mm film	52
Table 3.8	Constant parameters for synthesis LDPE composite film	53
Table 3.9	Variation in photocatalyst concentration in LDPE composites with two different thickness (0.1 mm and 0.035 mm)	53
Table 3.10	Constant parameters of UV reactor.....	63
Table 4.1	Average size of the particle of all photocatalysts measured using J image software	70
Table 4.2	Optical bandgap energies of synthesized photocatalyst.....	70
Table 4.3	Degradation percentage of MB and rate constant derived under pseudo first order reaction kinetics.	74
Table 4.4	Optical bandgap of each sample evaluated from trendlines inserted in $[F(R) \cdot hv]^{1/2}$ vs hv and $[F(R) \cdot hv]^2$ vs hv plots.....	80

Table 4.5	Degradation percentage of MB and rate constant of sample C-3ZT with different g-C ₃ N ₄ loading.	83
Table 4.6	DSC characteristics of LDPE and LDPE composites	94
Table 4.7.	Tensile properties of low density polyethylene (LDPE) samples with photocatalyst (10C-3ZT).....	100
Table 4.8	Degradation percentage, carbonyl index, degradation rate of the 1 mm polymer composite film after accelerated weathering test	103
Table 4.9	DSC characteristics of pure LDPE and LDPE composites with 0.1 mm thickness.....	109
Table 4.10	DSC characteristics of pure LDPE and LDPE composites with 0.035 mm thickness.....	109
Table 4.11	Tensile properties of 0.1 mm LDPE films with various amount of 10C-3ZT photocatalyst.....	123
Table 4.12	Tensile properties of 0.035 mm LDPE films with various amount of 10C-3ZT photocatalyst	123
Table 4.13	Weight loss, carbonyl index and degradation rate of the 0.1 mm polymer composite film after UV irradiation of 350 h	127
Table 4.14	Weight loss, carbonyl index and degradation rate of the 0.035 mm polymer composite film after UV irradiation of 350 h	127
Table 4.15	•OH, scavenging activity, O ₂ ^{•-} scavenging activity , h ⁺ scavenging activity of 0.1 mm and 0.035 mm films	132

LIST OF FIGURES

Figure 2.1	Polymer production by polymer category (Geyer et al., 2017).....	11
Figure 2.2	Cumulative plastic waste generation and disposal (in million metric tons). Solid lines show historical data from 1950 to 2015; dashed lines show projections of historical trends to 2050 (Geyer et al., 2017).....	11
Figure 2.3	One-electron reduction steps of oxygen to OH radical and two-electron oxidation step of water to H ₂ O ₂ observed in the TiO ₂ photocatalyst (Nosaka and Nosaka, 2013).	21
Figure 2.4	Mechanism Photooxidation in Polyethylene (Yousif and Haddad, 2013).	22
Figure 2.5	Using energy from light, TiO ₂ creates two oxidation reactants: hydroxyl radicals (•OH) and superoxide anion (O ₂ ^{•-}) which decomposes toxic organic substance by oxidation (Ibhadon and Fitzpatrick, 2013).	24
Figure 2.6	Schematic mechanism representation showing electron/hole separation process at coupled ZnO-TiO ₂ heterojunction interface (Hussein et al., 2013).	26
Figure 2.7	Mechanism of ZnO/g-C ₃ N ₄ (Sun et al., 2012).	29
Figure 2.8	Mechanism of g-C ₃ N ₄ /TiO ₂ (Miranda et al., 2013).....	30
Figure 3.1	Flowchart of the overall experiment.	44
Figure 3.2	Flowchart of the ZnO photocatalyst preparation.	46
Figure 3.3	Flowchart of the TiO ₂ photocatalyst preparation.	47
Figure 3.4	Flowchart of the ZnO/TiO ₂ photocatalyst preparation.....	48
Figure 3.5	Calcination profile of photocatalyst at 500°C.....	49
Figure 4.1	XRD diffractograms of photocatalysts (a), TiO ₂ . (b), Z3T. (c), ZT. (d), 3ZT. (e), ZnO. Where; ▲ is anatase, ▼ is rutile, ● is h-ZnTiO ₃ , ■ is c-Zn ₂ Ti ₃ O ₈ and ● is pristine ZnO. (h-ZnTiO ₃ : hexagonal-ZnTiO ₃ ; c-Zn ₂ Ti ₃ O ₈ :cubic-Zn ₂ Ti ₃ O ₈)	67
Figure 4.2	Morphological investigations via FESEM. (a), TiO ₂ . (b), Z3T. (c), ZT. (d), 3ZT. (e), ZnO photocatalysts synthesized by sol-gel and calcined at 500 °C.	69

Figure 4.3	Bandgap evaluations with UV-Vis spectroscopy. (a), Diffused reflectance spectra of 3ZT and ZnO photocatalyst and (b) Direct band gap obtained from Plot of $[F(R)hv]^2$ vs hv	71
Figure 4.4	Bandgap evaluations with UV-Vis spectroscopy. (a), Diffused reflectance spectra of ZT, 3ZT, and TiO_2 photocatalyst and (b) Indirect band gap obtained from Plot of $[F(R)hv]^{1/2}$ vs hv	72
Figure 4.5	Degradation of MB dye solution under sunlight using different composition of photocatalysts. (a), Plot of degradation percentage versus time. (b), Plot of $\ln(C_0/C)$ versus time. (a, \blacktriangle TiO_2 b, \blacktriangledown 3ZT c, \blacklozenge ZT d, \blacksquare 3ZT and e, \bullet ZnO).	73
Figure 4.6	(a) HRTEM and (b) enlarged HRTEM image of $3ZnO/c-Zn_2Ti_3O_8$ heterostructured particles, (c) The lattice plane spacing of 0.52 nm matched the (0001) planes of the zincite ZnO structure, (d) The lattice plane spacing of 0.58 nm matched the (110) planes of the c- $Zn_2Ti_3O_8$, (e) TEM image, (f) Zn element map, (g) O element map, (h) Ti element map, (i) the corresponding EDS recorded on the particles.	76
Figure 4.7	XRD of g- C_3N_4 /- $3ZnO$ -c- $Zn_2Ti_3O_8$ photocatalysts (a), g- C_3N_4 (b), 3ZT (c), 5C-3ZT (d), 10C-3ZT (e), 15C-3ZT (f), 20C-3ZT and (g), 25C-3ZT. (Where; \star is g- C_3N_4 , \blacksquare is c- $Zn_2Ti_3O_8$, and \bullet is pristine ZnO).	78
Figure 4.8	(a), UV-vis diffused reflectance spectra (DRS) of photocatalyst of g- C_3N_4 -3ZT composite with different percentage of g- C_3N_4 (5 wt%, 10 wt%, 15 wt%, 20 wt%, 25 wt%), 3ZT, and g- C_3N_4 . (b) Bandgap evaluations with UV-Vis spectroscopy. Plot of $[F(R)hv]^{1/2}$ vs hv of g- C_3N_4 , 5C-3ZT, 10C-3ZT, 15C-3ZT, 20C-3ZT, 25C-3ZT photocatalyst and (c) Direct band gap obtained from Plot of $[F(R)hv]^2$ vs hv of 3ZT photocatalyst.	80
Figure 4.9	Degradation percentage of MB in C-3ZT composite with different loading of g- C_3N_4	82
Figure 4.10	Degradation of methylene blue dye solution under sunlight in g- C_3N_4 -3ZT composite using different wt% of g- C_3N_4 . (a), Plot of degradation percentage versus time. (b), Plot of $\ln(C_0/C)$ versus	

	time. (a. ■ 10C-3ZT, b. ● 15C-3ZT, c. ▲ 20C-3ZT, d. ▼ 25C-3ZT, and e. ◆ 5C-3ZT).	82
Figure 4.11	Comparison of the MB degradation percentage according to the reusability of 10C-3ZT photocatalyst for five utilizations, after 45 min of exposition to sunlight.	83
Figure 4.12	XPS spectra of 10C-3ZT. (a), Survey spectra (b), C1s spectra (c), N1s (d), Ti2p (e), O1s and (f), Zn2p spectra.....	85
Figure 4.13	(a-d) HRTEM image of 10C-3ZT (10 wt% of g-C ₃ N ₄) photocatalyst.	87
Figure 4.14	(a) TEM image, (b) C element map, (c) N element map, (d) O element map, (e) Zn element map, (f) Ti element map.....	87
Figure 4.15	Schematic illustration of the proposed mechanism of electron-hole separation and transport and photocatalytic activity of (a) 3ZnO-c-Zn ₂ Ti ₃ O ₈ (b) g-C ₃ N ₄ /-3ZnO-c-Zn ₂ Ti ₃ O ₈ photocatalyst under ultraviolet and visible-light irradiation (sunlight).	89
Figure 4.16	PL-TA spectra of 3ZT and 10C-3ZT photocatalysts. Inset part in figure was the PL spectra changing with UV-vis light irradiation time for the case of the 10C-3ZT photocatalysts: (a), 0 min. (b), 15 min. (c), 30 min and (d), 45 min.	90
Figure 4.17	Appearance of 1 mm film (a) pure LDPE and LDPE composites with different wt% of 10C-3ZT (b), 0.1 wt% (c), 0.25 wt% (d), 0.5 wt% (e), 1 wt% photocatalyst.	92
Figure 4.18	XRD Spectra of (a) pure LDPE, LDPE composites with different wt% (b), 0.1 wt% (c), 0.25 wt% (d), 0.5 wt% (e), 1 wt%, with 1 mm thickness and photocatalyst species (f) 10C-3ZT, (g) g-C ₃ N ₄ . (Where; ▲ is PE; ★ is g-C ₃ N ₄ ; ● is ZnO ; ■ is c-Zn ₃ Ti ₂ O ₈).....	93
Figure 4.19	FESEM image of 1 mm pure LDPE and LDPE composites fracture surface before and after degradation under UV irradiation; (a),(b) pure LDPE, (c),(d) LDPE/10C-3ZT-0.1 wt%, (e),(f) LDPE/10C-3ZT-0.25 wt%, (g),(h) LDPE/10C-3ZT-0.5 wt%, and (i),(j) LDPE/10C-3ZT-1 wt%.	95
Figure 4.20	FTIR Spectra of 1 mm films before UV irradiation for (a) pure LDPE, (b) LDPE/10C-3ZT-0.1 wt%, (c) 0.25 wt%, (d) 0.5 wt%, and (e) 1 wt%.	97

Figure 4.21	FTIR Spectra of 1 mm films after UV irradiation for (a) pure LDPE, (b) LDPE/10C-3ZT-0.1 wt%, (c) 0.25 wt%, (d) 0.5 wt%, and (e) 1 wt%.	98
Figure 4.22	Stress-strain curves of 1 mm films (a) before UV irradiation and (b) after UV irradiation for pure LDPE, LDPE/10C-3ZT-0.1 wt%, 0.25 wt%, 0.5 wt%, and 1 wt%.	101
Figure 4.23	Carbonyl Index (CI) of various LDPE and composites film with 1 mm.	102
Figure 4.24	Colour change of 0.1 mm LDPE composite films with (a) 0 wt%, (b) 1 wt%, (c) 2 wt%, (d) 4 wt%, (e) 6 wt%, (f) 8 wt%, (g) 10 wt% photocatalyst of 10C-3ZT.	104
Figure 4.25	Colour change of films with 0.035 mm thickness (a) pure LDPE and LDPE/10C-3ZT- (b) 1 wt%, (c) 2 wt%, (d) 4 wt%, (e) 6 wt%, (f) 8 wt%, (g) 10 wt% photocatalyst of 10C-3ZT.	105
Figure 4.26	XRD spectra of 0.1 mm films (a) pure LDPE, (b) LDPE/10C-3ZT- 1 wt%, (c) LDPE/10C-3ZT-2 wt%, (d) LDPE/10C-3ZT-4 wt%, (e) LDPE/10C-3ZT-6 wt%, (f) LDPE/10C-3ZT-8 wt%, (g) LDPE/10C-3ZT-10 wt%, (h) 10C-3ZT, and (i) g-C ₃ N ₄ . (Where; ▲ is PE ; ● is ZnO; ★ is g-C ₃ N ₄)	107
Figure 4.27	XRD spectra of 0.035 mm films (a) pure LDPE, (b) LDPE/10C-3ZT-1 wt%, (c) LDPE/10C-3ZT-2 wt%, (d) LDPE/10C-3ZT-4 wt%, (e) LDPE/10C-3ZT-6 wt%, (f) LDPE/10C-3ZT-8 wt%, (g) LDPE/10C-3ZT-10 wt%, (h) 10C-3ZT and (i) g-C ₃ N ₄ . (Where; ▲ is PE; ★ is g-C ₃ N ₄ ; ● is ZnO ; ■ is c-Zn ₃ Ti ₂ O ₈)	108
Figure 4.28	FESEM images of (a) pure LDPE, (b) LDPE/10C-3ZT-1 wt%, (c) LDPE/10C-3ZT-2 wt%, (d) LDPE/10C-3ZT-4 wt%, (e) LDPE/10C-3ZT-6 wt%, (f) LDPE/10C-3ZT-8 wt%, (g) LDPE/10C-3ZT-10 wt%, before exposure. (Thickness: 0.1 mm) ...	112
Figure 4.29	FESEM images of (a) pure LDPE, (b) LDPE/10C-3ZT-1 wt%, (c) LDPE/10C-3ZT-2 wt%, (d) LDPE/10C-3ZT-4 wt%, (e) LDPE/10C-3ZT-6 wt%, (f) LDPE/10C-3ZT-8 wt%, (g) LDPE/10C-3ZT-10 wt% and inset exhibit the wide of the crack, after UV exposure. (Thickness: 0.1 mm)	113

Figure 4.30	FESEM images of (a) pure LDPE, (b) LDPE/10C-3ZT-1 wt%, (c) LDPE/10C-3ZT-2 wt%, (d) LDPE/10C-3ZT-4 wt%, (e) LDPE/10C-3ZT-6 wt%, (f) LDPE/10C-3ZT-8 wt%, (g) LDPE/10C-3ZT-10 wt%, before exposure. (Thickness: 0.035 mm)	114
Figure 4.31	FESEM images of (a) pure LDPE, (b) LDPE/10C-3ZT-1 wt%, (c) LDPE/10C-3ZT-2 wt%, (d) LDPE/10C-3ZT-4 wt%, (e) LDPE/10C-3ZT-6 wt%, (f) LDPE/10C-3ZT-8 wt%, (g) LDPE/10C-3ZT-10 wt%, after UV exposure. (Thickness: 0.035 mm)	115
Figure 4.32	FTIR Spectra of 0.1 mm films (A) before (B) after UV irradiation for (a) pure LDPE, (b) LDPE/10C-3ZT-1 wt%, (c) LDPE/10C-3ZT-2 wt%, (d) LDPE/10C-3ZT-4 wt%, (e) LDPE/10C-3ZT-6 wt%, (f) LDPE/10C-3ZT-8 wt%, (g) LDPE/10C-3ZT-10 wt%.	118
Figure 4.33	FTIR Spectra of 0.035 mm films (A) before (B) after UV irradiation for (a) pure LDPE, (b) LDPE/10C-3ZT-1 wt%, (c) LDPE/10C-3ZT-2 wt%, (d) LDPE/10C-3ZT-4 wt%, (e) LDPE/10C-3ZT-6 wt%, (f) LDPE/10C-3ZT-8 wt%, (g) LDPE/10C-3ZT-10 wt%.	120
Figure 4.34	Stress-strain curves: (a) before UV (b) after UV for 0.1 mm films and (c) before UV (d) after UV for 0.035 mm of pure LDPE, LDPE/10C-3ZT-1 wt%, LDPE/10C-3ZT-2 wt%, LDPE/10C-3ZT-4 wt%, LDPE/10C-3ZT-6 wt%, LDPE/10C-3ZT-8 wt%, LDPE/10C-3ZT-10 wt%.	124
Figure 4.35	Carbonyl Index (CI) of 0.1 mm for pure LDPE, LDPE/10C-3ZT-1 wt%, LDPE/10C-3ZT-2 wt%, LDPE/10C-3ZT-4 wt%, LDPE/10C-3ZT-6 wt%, LDPE/10C-3ZT-8 wt%, LDPE/10C-3ZT-10 wt% after UV irradiation.....	125
Figure 4.36	Carbonyl Index (CI) of 0.035 mm for pure LDPE, LDPE/10C-3ZT-1 wt%, LDPE/10C-3ZT-2 wt%, LDPE/10C-3ZT-4 wt%, LDPE/10C-3ZT-6 wt%, LDPE/10C-3ZT-8 wt%, LDPE/10C-3ZT-10 wt% after UV irradiation.....	125

Figure 4.37	Absorption percentage of MB of pure LDPE, LDPE/10C-3ZT-1 wt%, 2 wt%, 4 wt%, 6 wt%, 8 wt%, 10 wt% composites in dark region for 0.1 mm and 0.035 mm films.	128
Figure 4.38	Photocatalytic degradation of MB by pure LDPE, LDPE/10C-3ZT-1 wt%, 2 wt%, 4wt%, 6wt%, 8wt%, 10wt% composites under dark and UV light for 0.1 mm and 0.035 mm films.....	129
Figure 4.39	Influence of radical scavengers on the photodegradation of MB over LDPE, LDPE/10C-3ZT-1 wt%, 2 wt%, 4 wt%, 6 wt%, 8 wt%, 10 wt% composites, under UV light: Control (LDPE composite with MB alone), BQ as scavenger for $O_2^{\cdot-}$, MeOH as scavenger for h^+ , ACN scavenger for $\bullet OH$ for 0.1 mm films.....	131
Figure 4.40	Influence of radical scavengers on the photodegradation of MB over LDPE, LDPE/10C-3ZT-1 wt%, 2 wt%, 4 wt%, 6 wt%, 8 wt%, 10 wt% composites, under UV light: Control (LDPE composite with MB alone), BQ as scavenger for $O_2^{\cdot-}$, MeOH as scavenger for h^+ , ACN scavenger for $\bullet OH$ for 0.035 mm films.....	131
Figure 4.41	Photodegradation mechanism of LDPE composites films loaded with 10C-3ZT photocatalyst.	134
Figure 4.42	Photograph images of the (a), pure LDPE. (b), LDPE/10C-3ZT-10 wt% and (c), LDPE/10C-3ZT-10 wt%-PVA film before UV exposure.	136
Figure 4.43	Photograph images of the (a), pure LDPE (b), LDPE/10C-3ZT-10 wt% and (c), LDPE/10C-3ZT-10 wt%-PVA film after 350 h of UV exposure.	136
Figure 4.44	FESEM images of the (a), pure LDPE (b), LDPE/10C-3ZT-10 wt% and (c), LDPE/10C-3ZT-10 wt%-PVA film before UV exposure.	137
Figure 4.45	FESEM images of the (a), pure LDPE (b), LDPE/10C-3ZT-10 wt% and (c), LDPE/10C-3ZT-10 wt%-PVA film after 200 h of UV exposure.	138
Figure 4.46	Percentage of water gain in (a) pure LDPE, (b) LDPE/10C-3ZT-10 wt%, and (c) LDPE/10C-3ZT-10 wt %-PVA as a function of soaking duration.	139

Figure 4.47	Schematic diagram of reaction between PVA and $\text{OH}\cdot$ which facilitate LDPE degradation.	140
Figure 4.48	FTIR spectrum of (a) pure LDPE, (b) LDPE/10C-3ZT-10 wt%, and (c) LDPE/10C-3ZT-10 wt%-PVA before degradation.	142
Figure 4.49	FTIR spectrum of (a) pure LDPE, (b) LDPE/10C-3ZT-10 wt%, and (c) LDPE/10C-3ZT-10 wt%-PVA after degradation.	143
Figure 4.50	Absorption and photodegradation of MB for LDPE/10C-3ZT-10 wt%-PVA composite under dark and UV light: Dark (LDPE composite in MB without UV and scavenger), MB (LDPE composite with MB alone), ACN scavenger for $\cdot\text{OH}$, BQ as scavenger for $\text{O}_2^{\cdot-}$, MeOH as scavenger for h^+	145
Figure 4.51	Weight loss of 0.035 mm of pure LDPE, LDPE/10C-3ZT-10 wt%, and LDPE/10C-3ZT-10 wt%-PVA after 350 hours irradiation.	146
Figure 4.52	Carbonyl Index (CI) of 0.035 mm of pure LDPE, LDPE/10C-3ZT-10wt%, and LDPE/10C-3ZT-10 wt%-PVA after 350 hours irradiation.	146

LIST OF SYMBOLS

$^{\circ}\text{C}$	Degree Celsius
θ	Angle
%	Percentage
g	Gram
h	Hour
min	Minutes
ml	Milliliter
nm	Nanometer
ppm	Parts per million
rpm	Revolution per minute
e^{-}	Electron
h^{+}	Hole

LIST OF ABBREVIATIONS

CB	Conduction band
CI	Carbonyl Index
10C-3ZT	10g-C ₃ N ₄ -3ZnO-c-Zn ₂ Ti ₃ O ₈
10C-3ZT-PVA	10g-C ₃ N ₄ -3ZnO-c-Zn ₂ Ti ₃ O ₈ -Polyvinyl Alcohol
EDX	Energy dispersive X-ray Spectroscopy
FESEM	Field-Emission Scanning Electron Microscopy
FTIR	Fourier Transform Infrared Spectroscopy
HRTEM	High Resolution Transmission Electron Microscopy
ICDD/ J	International Centre for Diffraction Data
LDPE	Low density Polyethylene
MB	Methylene blue
HO•	Hydroxyl radical
VB	Valence band
PE	Polyethylene
PP	Polypropylene
PS	Polystyrene
TTIP	Titanium (IV) isopropoxide
UV	Ultraviolet
UV-vis	UV-Visible spectroscopy
ZAD	Zinc acetate dihydrate

PRESTASI FOTODEGRADASI KOMPOSIT POLIETILENA
BERKETUMPATAN RENDAH DENGAN PENAMBAHAN FOTOMANGKIN

ABSTRAK

Peningkatan pengeluaran dan penggunaan plastik di seluruh dunia menyebabkan sisa pepejal yang ketara dan masalah pencemaran yang serius. Pelbagai pendekatan telah diambil dan fotodegradasi merupakan satu pendekatan yang mesra alam sekitar. Walau bagaimanapun, kadar degradasi yang telah dicapai hanya dalam lingkungan, 0.03-0.21 %/h. Oleh itu, dalam kajian ini, katalis yang sesuai dan boleh mempercepatkan kadar degradasi polimer telah dibangunkan menggunakan zink oksida (ZnO), titanium dioksida (TiO₂) dan karbon nitrida grafitik (g-C₃N₄) melalui kaedah larutan gel. Kesan nisbah ZnO/TiO₂ dan peratus berat g-C₃N₄ dikaji. Fotokatalis ZnO/TiO₂ dengan nisbah 3: 1 bersama 10% berat g-C₃N₄ yang dinamakan 10C-3ZT dan mempunyai aktiviti fotokatalis yang tertinggi dipilih untuk membangunkan filem komposit LDPE. 10C-3ZT merupakan fotokatalis yang optimum dengan ciri-ciri berikut; didominasi oleh fasa zinksit dan pembentukan struktur hetero di antara ZnO/g-C₃N₄ dan c-Zn₂Ti₃O₈/g-C₃N₄, campuran zarah berbentuk sfera dan rod, jurang tenaga yang rendah 2.5 eV merendahkan kadar penggabungan semula e-h dan menyebabkan kadar fotodegradasi sebanyak 99% dalam tempoh 45 minit dengan pemalar kadar kinetik 0.093 min⁻¹. Filem komposit LDPE dengan 3 ketebalan yang berbeza (1 mm, 0.1 mm dan 0.035 mm) telah disediakan dengan 10C-3ZT. Pengacuan mampatan telah digunakan untuk menghasilkan 1 mm filem komposit dan kaedah pengacuan basah untuk menghasilkan filem dengan ketebalan 0.1 dan 0.035 mm. Peratus berat 10C-3ZT telah diubah dari 1

hingga 10% berat dan sifat-sifat filem komposit LDPE/10C-3ZT dibandingkan dengan LDPE tulen dengan menganalisis perubahan berat, indeks karbonil, kekuatan tegangan, pemanjangan, morfologi, struktur kimia dan darjah penghabluran. Kehilangan berat dipertingkatkan dengan menambah 10% berat PVA (10C-3ZT-10 wt%-PVA) dalam matriks polimer LDPE. Pengurangan berat filem sebanyak 96% telah dicapai dalam masa 350 h. Indeks karbonil sehingga 2 telah dicapai. Pembebasan OH• disebabkan pembentukan sturuktur hetero, peningkatan fasa amorfus dan kebolehan PVA untuk menyerap air telah menyebabkan degradasi LDPE menjadi ketara, dimana 47 kali lebih cepat daripada LDPE tulen.

PHOTODEGRADATION PERFORMANCES OF LOW-DENSITY POLYETHYLENE COMPOSITES LOADED WITH PHOTOCATALYSTS

ABSTRACT

Growing production and consumption plastic worldwide is currently resulting in a significant solid waste and is causing serious pollution problems. Various approach has been attempted and photodegradation seems to be the environmental benign approach. However, the degradation rate that has been achieved is only in the range of 0.03 to 0.21 %/h. Therefore, in this work, an appropriate photocatalyst that could expedite the photodegradation rate of the polymer was developed based on zinc oxide (ZnO), titanium dioxide (TiO₂) and graphitic carbon nitride (g-C₃N₄) by sol gel method. The effect of ZnO/TiO₂ ratio and wt% of g-C₃N₄ was investigated. The best photocatalytic activity performed by photocatalyst ZnO/TiO₂ with ratio of 3:1 that was incorporated with 10 wt% g-C₃N₄ denoted as 10C-3ZT was selected to fabricate LDPE composite films. The optimized photocatalyst is 10C-3ZT with following features: dominated by zincite phase and minor traces of c-Zn₂Ti₃O₈ together g-C₃N₄, formation of heterojunctions within ZnO/g-C₃N₄ and c-Zn₂Ti₃O₈/g-C₃N₄, mixture of spherical and rod shape particles, low band gap energy of 2.5 eV have remarkable reduced recombination of e-h in 10C-3ZT photocatalyst thus resulted in 99% degradation within 45 minutes with kinetic rate constant of 0.093 min⁻¹. LDPE composite films with 3 different thickness (1 mm, 0.1 mm and 0.035 mm) was prepared with 10C-3ZT. Compression moulding was used to produce 1 mm composite films and wet casting method for films with 0.1 and 0.035 mm thickness. The weight % of 10C-3ZT was varied from 1 to 10 wt% and the properties of LDPE/10C-3ZT composite films were

compared with pure LDPE by analysing the changes in weight loss, carbonyl index, tensile strength, percentage elongation, morphology, chemical structure, degree of crystallinity. The weight loss was further enhanced with 10 wt% PVA functionalized photocatalyst (10C-3ZT-10 wt%-PVA) in LDPE polymer matrix. The total weight loss of 96% was attained in 350 h. Carbonyl index up to 2 was achieved. Enhanced OH• released due to heterostructure formation, increase in amorphous region and PVA functionalization for water absorption resulted in substantially improvement in degradation of LDPE, which was 47 times faster than pure LDPE.

CHAPTER 1

INTRODUCTION

1.1 Research Background

Polymers are very versatile materials that enable many applications to be realized due to their excellent properties in flexibility, hardness, lightness, barrier against the permeation of gases, and low cost (Azlin-Hasim et al., 2016; Gaska et al., 2017; Aldas et al., 2018; Arráez et al., 2019). The use of polymer in several applications such as packaging, biomedical products and disposal items, auto parts, clothing, toys, etc has become a topic of fundamental importance in terms of its impact to the environment benign due to accumulation of plastic waste that is difficult to degrade (Singh and Sharma, 2008; Sevigné-Itoiz et al., 2015; Shen et al., 2018). United Nations Program for the Environment (UNEP) had reported that 12.5% of the municipal solid waste (MSW) generated around the world is contributed by plastics. This is equivalent to roughly 25 million tons of waste produced per year and 50% of this amount comes from packaging, such as polyethylene (PE), low density polyethylene (LDPE) and linear low density polyethylene (LLDPE) (Portillo et al., 2016).

Current disposal technology available to overcome these polymer wastes problems are landfill, incineration, and recycling. Among all, landfill is the major approach used for waste management in Malaysia as well as through worldwide. Approximately 75.4 – 95.0 percent of waste collected is taken to landfill sites for disposal and the remaining waste is either sent to incineration plants or diverted to recyclers (Moh, 2017). Nevertheless, dispose of plastic by landfill method results in persistent organic pollutants production and requires more space (Moh and Manaf,

2014). Incineration is a good potential option to dispose plastic waste instead of landfill. However, it is costly and requires technological experts to operate it (Trindade et al., 2018). In that case, recycling of plastic product to manufacture a new product would be an environmentally friendly approach to handle plastic waste, for example, thermoplastics can be re-melted and reused, and thermoset plastics can be ground up and used as a filler, although the quality of the material tends to degrade with each reuse cycle. Thus, the limitation of the current disposal technology has triggered lots of researchers to develop eco-friendly and cost-effective methods to address the plastics waste disposal. Degradation of plastic waste through various means such as thermal degradation (He and Ma, 2015; Choong and De Focatiis, 2016; Herrera-Kao et al., 2018), biodegradation and photodegradation (Gårdebjer et al., 2015; Zenteno et al., 2017; Wilkes and Aristilde, 2017; Johnston et al., 2017; Ahmed et al., 2018), has become alternatives to deal with the plastic waste.

Thermal degradation of polyethylene plastics waste into fuel oils was investigated by Rolón-Garrido et al. (2011). Nonetheless, this technique requires not only high temperature (170°C - 360°C) and cost of roughly \$0.19-1.31/ton CO₂ (Davis and Rochelle, 2009), but also appropriate catalysts to guarantee narrow distribution of hydrocarbons (Zhao et al., 2007). Biodegradable plastics also seen as solution as these plastics will degrade within 50 - 120 days but it scares the food security for the resources are from plant base such as benzene. Thus, attention has been focused on photodegradation because it is one of the environmental benign method to tackle plastic waste problem. It is a method whereby the polymer decompose by the action of ultraviolet or visible light being absorbed by the polymer chain itself thus produce by-product such as ketone, ester, carbocyclic acid which further decompose with time to produce carbon dioxide and water.

Plastics such as polyethylene (PE), polystyrene (PS) and polypropylene (PP) cannot initiate the photodegradation itself under UV radiation and visible light as they do not contain groups that are capable to absorb in the UV spectrum (Yousif and Haddad, 2013; Canopoli et al., 2018). Therefore, impurity doping using metal (Yusak et al., 2015; Low et al., 2017), metal-transition (Montagna et al., 2015), non-metal or metal oxide (Ali et al., 2016; Das et al., 2017) photocatalysts may be used to facilitate the photodegradation of plastics. Photocatalyst absorbs light radiation and creates electron-hole pairs which are utilized in the generation of free radicals such as $O_2^{\cdot-}$, HOO^{\cdot} and OH^{\cdot} (HO^{\cdot}). These active radicals or reactive oxygen species (ROS) are able to oxidize the C-H bond (UVB= 253-315 nm, 413 kJ) which leads to the degradation of the organic molecule (Suzuki et al., 2015). The free radicals initiate the oxidation mechanisms of photodegradation process, which is known as Advanced Oxidation Process (AOP).

Various works on AOP using various photocatalysts in different types of polymer photocatalyst by far are dominated by TiO_2 . However, this polymer possesses low degradation property. The reason for its low degradation rate is perhaps due to the choice of using single oxide photocatalyst in polymer composites oxide (eg. TiO_2 or ZnO). The drawbacks of using single oxide photocatalyst in polymer can be explained as follows: i) single oxide photocatalyst has high e-h recombination rate (ii) single oxide photocatalyst has small surface area which in turn decreases the interface area between single oxide (eg. TiO_2 or ZnO) and LDPE matrix (Yang et al., 2011; Alvarado et al., 2016) and clearly, the decreased interface area, due to small surface area, between single oxide and LDPE polymer matrix tends to lower the production of OH^{\cdot} radical (OH^{\cdot}), and, iii) single oxide (eg. TiO_2 and ZnO) has large band gap and is active in UV region, resulting in low photodegradation rate.

To overcome the problems, coupled oxides 10C-3ZT were selected and developed by sol-gel method to form heterojunction that limit e-h recombination rate, and to enhance water absorption by PVA functionalization to increase the production of OH radical ($\text{OH}\cdot$), resulting in high photodegradation rate. Therefore, in this thesis, the latest updates on photodegradable characteristic of LDPE composite film using 1, 2, 4, 6, 8, 10 wt% 10C-3ZT coupled oxides and correlation within the structural, thermal, tensile and degradation properties are reported.

1.2 Problem Statement

Although photodegradation is an environmentally friendly treatment, the widespread use was hindered due to several limitations.

a) High Recombination of electron-hole (e-h), large bandgap and low visible light response

In the last few years, common semiconducting oxides such as titanium dioxide (TiO_2) (Ali et al., 2016; Alvarado et al., 2016) and zinc oxide (ZnO) were used to degrade polymer due to their chemical stability (Cai et al., 2017; Liu et al., 2017b), atoxic properties (Yousefi et al., 2015; Khaki et al., 2017; Cai et al., 2017)), low cost (Saeedi et al., 2015; Marimuthu et al., 2016), and anti-pathogen activity (Tahir et al., 2015). The percentages of photocatalysts added were in the range of 1 to 20 wt% with average photodegradation rate of 0.03 to 0.21 %/h. The highest carbonyl index attained was approximately 2, under UV irradiation only after 15 days of degradation, which is considered low (Ali et al., 2016). The reason for their low degradation rate perhaps is due to the choice of using single oxide photocatalyst (eg. TiO_2 or ZnO) in polymer. Major drawback of using single oxide photocatalyst in polymer is the high e-h

recombination rate of single oxide photocatalyst, which recombines more rapidly than surface redox reactions. Single oxide photocatalyst such as TiO_2 and ZnO which is largely utilized for polymer photodegradation studies has a large band gap energy, which is 3.2 eV and 3.37 eV, respectively (Hosseini et al., 2015; Akir et al., 2016; Alibe et al., 2017; Habba et al., 2017; Romero Saez et al., 2017; Bodke et al., 2018; Ashebir et al., 2018; López et al., 2019). Therefore, the excitation can only be expedited by supplying UV light, thus deteriorate the polymer degradation rate. The use of visible light species such as g- C_3N_4 on ZnO/TiO_2 coupled oxides heterostructure photocatalyst to extend the visible light respond and limit the electron-hole pair recombination, thus improving the degradation rate were used as a photocatalyst to be incorporated into the LDPE matrix.

b) Thickness problem of photodegradable polyethylene (PE)

Polymer thickness that used varies with different application. Most of the packaging material range from 0.024 - 0.1 mm. Besides, it is also known that degradation of a polymer also influenced by the thickness. It was found the degradation rate are in 0.03 - 0.21%/h when thickness varies from 0.024 - 0.1 mm. Therefore, in this work, the different thicknesses of LDPE, 0.1 mm and 0.035 mm, are investigated. The polymer thickness was scaled down from 1 mm to 0.1 mm and 0.035 mm by wet casting method.

c) Poor water absorption

The hydrophobic properties of polymer, such as polyethylene, hinders water absorption into the bulk polymer matrix and makes the photocatalytic reaction preferably to occur at the polymer surface. Some studies showed that the introduction of hydrophilic polymer with multi-hydroxyl groups such as Poly (vinyl alcohol) (PVA)

into polymer composite can enhance the moisture/water absorption from atmosphere and thus produces more hydroxyl radicals to expedite polymer degradation (Kim et al., 2015). Therefore, in this work PVA functionalized photocatalyst was used to expedite the ROS formation and the polymer degradation process.

1.3 Research Objectives

This research is intended to synthesize high efficiency photocatalyst (PC) for high rate LDPE degradation. The main objectives of this research are described as follows;

1. To formulate and characterize a coupled oxide based photocatalyst with different ratio of ZnO and TiO₂ and modify with g-C₃N₄ to form a visible light photocatalyst with high photodegradation efficiency.
2. To investigate the effect of photocatalyst incorporation on structural, tensile, thermal and degradation properties of 1 mm, 0.1 mm and 0.035 mm films.
3. To investigate the effect of PVA functionalized photocatalyst on photodegradation properties of LDPE.

1.4 Research Scope

ZnO/TiO₂ photocatalyst was synthesized with mol ratio of 1:0, 3:1, 1:3, 0:1 by mixing TiO₂ sol and ZnO sol. The ZnO sol was then directly incorporated into TiO₂ sol to produce ZnO/TiO₂ composite sol. A mixture of 3ZnO/c-Zn₂Ti₃O₈ with g-C₃N₄ photocatalyst was prepared by grinding 5, 10, 15, 20, and 25 wt% of g-C₃N₄ together with 95, 90, 85, 80, and 75 wt% of 3ZnO/c-Zn₂Ti₃O₈ respectively using pestle and

agate mortar. To select the best photocatalyst, X-ray Diffraction (XRD), Field Emission Scanning Electron Microscopy (FESEM), Ultra Violet Diffuse Reflectance Spectroscopy (UV-DRS), High Resolution Transmission Electron Microscopy (HRTEM), X-ray Photoelectron Spectroscopy (XPS), photocatalytic activity tests and Photoluminescence Terephthalic Acid (PL-TA) measurement were carried out. The information on the crystal structure, surface morphology, optical band gap and photocatalytic activity, scavenger test was obtained to understand the high photocatalytic activity in the optimized sample (10C-3ZT).

After selecting the best photocatalyst from objective 1, LDPE composites films of 1 mm thickness was prepared by compression moulding method by varying the weight percentage of the photocatalyst from 0.1, 0.25, 0.5, 1 wt%. For 0.1 and 0.035 mm compression moulding was not suitable and therefore wet casting method was adopted. This is done by dissolving 0.5 g or 1 g of LDPE pellets and different wt% of photocatalyst in 20 ml 1,2 Dichlorobenzene (DCB) at 115-130 °C under continuous stirring with magnetic bar for 30 min. Prior to this, the required amount of photocatalyst was added into DCB containing LDPE pellets under ultrasonic vibration using ultrasonic bath for 30 min.

The LDPE solution was then poured into a petri dish to be left dry at 80 °C (thickness: 0.1 mm). Then, the same procedure was repeated for different thickness (0.035 mm) by reducing the mixture volume from 20 ml for 0.1 mm films to 6 ml for 0.035 mm films. To understand the photodegradation properties of LDPE composite film, various analysis such as XRD, FESEM, DSC, FTIR, tensile testing (tensile strength and percentage of elongation) were carried out. Since most application

including commodity plastic use thickness of 0.035 mm LDPE/10C-3ZT-0.035 mm was further modified with the addition of 10 wt% PVA to expedite the degradation.

1.5 Thesis Outline

This thesis is presented in 5 chapters. Chapter 1 introduces the information on the waste resulted from utilization of polymer materials and the limitation of available method to address the issues. It also provides justification on the photodegradation approach selected in this work. This is followed by the problem statement, objectives, scope of the research and research outline.

Chapter 2 provides reviews of the relevant literature. First section reviews on polymer waste generation statistic, the second section evaluates the current management technologies available to treat polymer waste and drawbacks of current plastic waste disposal. The third section elaborates on several other degradation methods on polyethylene (PE). The final section highlights factors that affects a polymer degradation process and the mechanism.

Chapter 3 details the information about the raw materials used in this study, experimental procedure or experimental design to synthesize photocatalyst. Brief explanation on the characterization techniques and photodegradation analysis is elucidated. Chapter 4 describes the experimental results and discussions on the synthesized photocatalysts (PCs), which were prepared by sol-gel method and their photodegradation rate performances. This is followed by characterization of LDPE composite films prepared by compression moulding method and wet casting method.

For compression moulding method, 10C-3ZT with different loadings (0, 0.1, 0.25, 0.5, 1 wt%) was selected to be further incorporated into LDPE with 1 mm

thickness and evaluated for photodegradation property. Then, LDPE/10C-3ZT composites films with thickness of 0.1 mm and 0.035 mm that were fabricated using wet casting method with and without PVA functionalization are attached. Chapter 5 provides the conclusions of the findings based on the objectives with few recommendations for the future work.

CHAPTER 2

LITERATURE REVIEW

This chapter presents the literature review of photocatalyst and LDPE-photocatalyst synthesized by sol-gel, compression molding and wet casting methods. This chapter is divided into four sections. The first section reviews polymer waste generation statistic, the second section evaluates current management technology available to treat polymer waste and drawbacks of current plastic waste disposal. The third section elaborates on several other degradation methods on polyethylene (PE). The fourth section highlights factors affecting photocatalyst and polymer degradation.

2.1 Polymer Waste Generation

Past 25 years, there has been a continuous increase in the manufacturing of commodity and packaging plastic production such as polyolefins. Polyethylene (PE) is one of the polyolefin material that largely consumed due to its high strength, good barrier properties, light weight, and higher stability (Onyshchenko et al., 2015; Geyer et al., 2017). In 2050, global plastic consumption is estimated to be 25,000 million metric ton and 37% are dominated by PE (Figure 2.1). Besides, the statistic in Figure 2.2 obviously shows that the continuous use of PE in packaging would lead to the generation of a large quantity of plastic waste every year. The accumulation of those plastic waste in environment would lead to long term environmental and waste management problems.

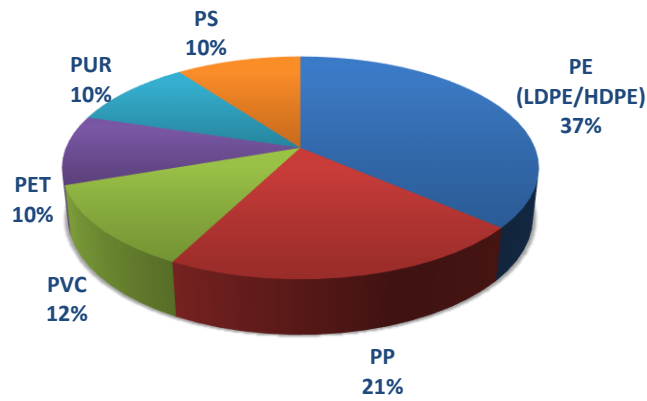


Figure 2.1 Polymer production by polymer category (Geyer et al., 2017).

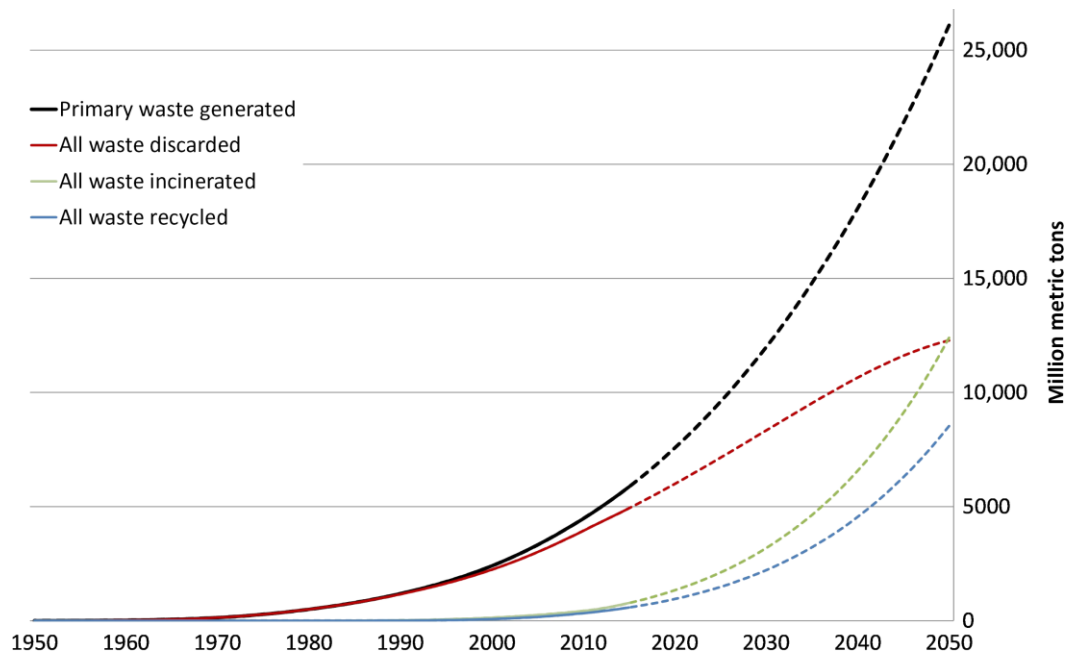


Figure 2.2 Cumulative plastic waste generation and disposal (in million metric tons). Solid lines show historical data from 1950 to 2015; dashed lines show projections of historical trends to 2050 (Geyer et al., 2017).

2.2 Current Waste Management Technologies

Current disposal technologies available to overcome the problems are landfill, incineration, and recycle. The details are discussed in the following section.

2.2.1 Landfill

Approximately 75.4- 95 percent of waste collected is taken to landfill sites for disposal and the remaining waste is either sent for incineration plants or diverted to recyclers (Moh, 2017). A landfill site (also known as a tip, dump, rubbish dump, garbage dump or dumping ground) is a site for the disposal of waste materials by burial. Modern landfills are well-engineered and managed facilities for the disposal of solid waste. Two main disadvantages of landfill method are the inconveniences caused by persistent organic pollutants and the requirement of more space (Moh and Manaf, 2014; Verma et al., 2016; Moh, 2017). When disposed in landfills, plastic waste creates soil and air pollution (Bhattacharjee and Bajwa, 2018; Joseph et al., 2018), since they are nonbiodegradable (do not decompose) under natural environmental condition (Li et al., 2016a). Other disadvantages include destruction of entire ecosystems, threatening animal life, high cost (Fa et al., 2016) namely \$ 78 in 2016, and a 2% average annual growth of cost (Watson, 2016).

2.2.2 Incineration

According to United States Environmental Protection Agency (EPA), 15.5% of plastic materials generated in the U.S. Municipal Solid Waste (MSW) stream was combusted for energy, while 75.4% was sent to landfills. Incineration is the process of destruction of waste in a furnace by controlled burning at high temperatures. It removes water from hazardous sludge, reduces its mass and/or volume, and converts it to a non-burnable ash that can be safely disposed of on land, in some waters, or in underground pits. Thus, incineration is another potentially good option to dispose plastic waste. An advantage of the incineration is that it reduces the weight and volume

of the waste resulting in a less hazardous amount of waste. The gas and residue that incineration produces, such as slag and ash, is odourless. Another advantage is that waste incineration requires less land area as compared to landfill method. However, it is costly and requires technological experts to operate it (Trindade et al., 2018). Municipal solid waste incinerators also normally include fuel gas treatments to reduce pollutants further as uncontrolled incineration of plastic produces polychlorinated dibenzo-p-dioxins, a carcinogen (cancer causing chemical). The issue of fuel gas treatments is the variation of the heat content of the waste stream (Ojha et al., 2017). Other disadvantages of incineration include the discharges of carcinogenic dioxin gas or noxious gas (Briassoulis, 2006; Thomas and Sandhyarani, 2013). Air pollution and ground contamination in the vicinity of such municipal facilities are observed. The emission of toxic gases also reported to cause global warming (Fa et al., 2008; Petchwattana et al., 2012; da Silva et al., 2015; Das et al., 2017; Bhattacharjee and Bajwa, 2018).

2.2.3 Recycling

Nine point one percent (9.1%) of plastic material generated in the U.S. Municipal Solid Waste (MSW) stream was recycled in 2015 (Wheeler, 2017). Recycling is the process of using recovered material to manufacture a new product. One of the plastic recycling challenge is the difficulty to sort the plastic wastes automatically, making it labour-intensive. Other recyclable materials such as metals are easier to process mechanically. However, new processes of mechanical sorting are required to increase capacity and efficiency of plastic recycling (Petchwattana et al., 2012). Advantages of recycling are that it is non-toxic, environmentally friendly method, a non- destructive process that can help reuse the material, a way to conserve

natural resources, and it is a more sustainable approach (da Silva et al., 2015; Mwanza and Mbohwa, 2017). However, a disadvantage of recycling is that the development of new processes of mechanical sorting, are not economically viable, time consuming, and energetically unviable (Fa et al., 2008; da Silva et al., 2015; Gu et al., 2017). The drawbacks of the current disposal technologies have triggered researchers to develop eco-friendly and cost-effective methods to address plastics waste disposal (Kyaw et al., 2012; Ojha et al., 2017). Degradation of plastic waste through various means such as thermal degradation (Francis, 2013; Arráez et al., 2018; Nakayama et al., 2017) and photodegradation (Bahrami et al., 2018) are a few alternative techniques to deal with plastic waste.

2.3 Several Other Degradation Methods on PE

There are polyethylene waste management methods such as thermal degradation (Neelam et al., 2018), biological degradation (by fungi, bacteria, yeasts, algae, enzymes) (Fa et al., 2016), and photodegradation (Singh and Sharma, 2008) have been reported but not widely applied to handle polymer waste due to certain limitations. A summary of various degradation methods is given in Table 2.1. The details, advantages and limitations of these techniques are discussed in the following subsections.

2.3.1 Thermal Degradation

Thermal degradation is the process of a polymer degradation because of the action of heat. The effects can be very different subjecting to the components of the polymer composite and, consecutively, on their chemical structure (La Mantia et al.,

2017). The thermal degradation rate of polymer directly determined by the temperature (Ammala et al., 2011).

Initially random scission was identified as the mechanism responsible for degradation of polyethylene. It was realized that two mechanisms occur simultaneously, namely chain scission and molecular enlargement, which cause an increase of the degree of side-chain branching. Kumar et al. (2002) reported the thermal degradation of LDPE in liquid paraffin for 3 hours at various temperatures of 280°C -360°C. The rate constant in the study were 0.49×10^{-7} , 15×10^{-7} and $74 \times 10^{-7} \text{ min}^{-1}$ for temperature 280°C, 340°C, and 360°C respectively, indicating that higher temperature performs faster reactions.

Cuadri and Martín-Alfonso (2017) studied the influence of thermal and thermo-oxidative degradation on the chemical, thermal property of high density polyethylene (HDPE) subjected to different degradation time, namely: 0, 10, 30 and 60 min at 150°C, 175°C, 200°C, 225°C. FTIR test revealed that there is an increase in carbonyl index (CI) values and the degraded products with increasing decomposition time and temperature (Table 2.1). Therefore, it can be concluded that the higher weight reduction of HDPE was observed for longer degradation time and temperature. Disadvantages of thermal degradation technique are the requirement of high temperature (170 - 360 °C) (Kumar et al., 2002; Sogancioglu et al., 2017; Cuadri and Martín-Alfonso, 2017), costly, namely \$0.19/ton CO₂ at the lower temperature and \$1.31/ton CO₂ at the higher temperature (Davis and Rochelle, 2009), and slightly toxic (Herrera-Kao et al., 2018).

Table 2.1 Summaries of polyethylene degradation methods

Degradation	Parameter (eg. Temperature, etc)	Weight loss, Yielded of degraded product	Degradation rate %/h	k	CI	Disadvantages	Ref
Thermal Degradation	Temperature: 280–360°C Dissolve in liquid paraffin	NA	NA	0.49×10^{-7}	NA	Slightly Toxic	(Kumar et al., 2002)
			NA	15×10^{-7}	NA		
			NA	74×10^{-7}	NA		
Thermal Degradation	Temperature: 200°C	NA	NA	NA	60 min; CI:5	Slightly Toxic	(Cuadri and Martín-Alfonso, 2017)
			NA	NA	30min; CI:2		
			NA	NA	10min; CI:1		
Biodegradation	Temperature: 40°C	NA	PM2>PM1	NA	PM2>PM1 CI>6	Long time to degrade	(Han et al., 2018)
Biodegradation	Control	Loss=0.3%	0.0025%/h	NA	NA	Long time to degrade	(Kyaw et al., 2012)
	<i>Psuedomonas aeruginosa</i> PAO1(B1)	Loss=20%	0.16%/h				
	<i>Psuedomonas aeruginosa</i> ATCC(B2)	Loss=11%	0.091%/h				
	<i>Pseudomonas putida</i> (B3)	Loss=9%	0.075%/h				
	<i>Pseudomonas syringae</i> (B4)	Loss=11.3%	0.094%/h				

2.3.2 Biodegradation

The development of biodegradable plastics is regarded as another ultimate solution to solve the environmental problem (Ge et al., 2017). Degradable PE plastic is prepared using additives, such as starch (Jiménez et al., 2016; Masmoudi et al., 2016; Muller et al., 2017), cellulose (Tan et al., 2015; Zhang et al., 2016; Pinheiro et al., 2017), lignin (Yang et al., 2015), and dextrin (Das et al., 2015), which increase the biodegradability. The biodegradation mechanism of PE involves two stages: 1) an abiotic (photo or thermo) oxidation and 2) a microbial biodegradation. Initial abiotic oxidation is important as it usually controls the entire degradation rate (Reddy et al., 2008; Zenteno et al., 2017). However, the fragmentation of PE, caused by degradation of starch and similar additives in the blends, causes recycling difficulties (Roy et al., 2011). Recently, Han et al. (2018) reported that nano-clay has been used as an additive in PE to improve the biodegradation of polymer. The degradation property for packaging material 2 (PM2) with a larger amount of nano-clays, was higher than that observed in packaging material 1 (PM1), suggesting that the presence of nano-clay in larger amount in PM2 accelerated the photodegradation more than PM1.

In general, the resistance of PE to biological attack was believed to be a reason for low degradation rate which is attributed to the hydrophobic and high molecular weight of the polymer. Several studies have investigated on biodegradation of polyethylene by bacterial and fungal species as microorganism for LDPE direct degradation. For instance *Pseudomonas spp.* degrade LDPE bags in natural and artificial environment (Roy et al., 2011; Kyaw et al., 2012). After 120 days, the weight loss and degradation rate have been reported to be 20% and 0.16 %/h in *Pseudomonas*

aeruginosa (B1), 11% and 0.091 %/h in *Pseudomonas aeruginosa* (B2), 9% and 0.075 %/h in *Pseudomonas Patida* (B3), 11.3% and 0.094 %/h in *Pseudomonas syringae* (B4), 0.3% and 0.0025 %/h for control. However, the degradation of polymer into monomer is a long term degradation since the disintegration of large polymers to carbon dioxide (CO₂) needs several different organisms, with one breaking down the polymer into its monomers (Yang et al., 2010; Kyaw et al., 2012; Vijayvargiya et al., 2014; Ojha et al., 2017) and it is costly.

2.3.3 Photodegradation

Photodegradation of plastics is another eco-friendly method, which is the process of polymer decomposition by the action of ultraviolet or visible light. The photodegradation may be induced by either the absorption of the light or photon by the polymer chain itself or by some photocatalysts incorporated in the polymer (Yousif and Haddad, 2013; Kulkarni and Dasari, 2018). Impurity incorporation such as metal (Asghar et al., 2011; Hosseini et al., 2015), metal-transition (Corti et al., 2010), non-metal or metal oxide photocatalyst (Yusoff et al., 2017) may be used to facilitate the photodegradation of plastics (Suzuki et al., 2015). The common semiconducting oxides used include titanium dioxide (TiO₂) and zinc oxide (ZnO) to degrade different types of polymer such as PE (Castillo-Reyes et al., 2019), PVC (Fa et al., 2011; Mallakpour and Shamsaddinimotlagh, 2018), and PS (Zan et al., 2006).

Photodegradation involves the natural tendency of most polymers composite to atmospheric oxygen in the presence of light. Normally, a photocatalyst is employed to light (UV) which then leads to the generation of free radicals. An auto-oxidation process then occurs, resulting in the eventual disintegration of the plastic. It is believed

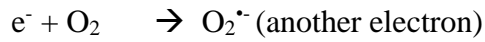
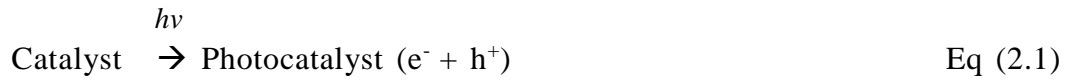
that the instability of polyolefins is caused by the presence of carbonyl and by hydroperoxide group (-CH-OOH). The mechanism of degradation of polyethylene proposed by Liu et al. (2011) describes the formation of carboxylic acids, peroxide, ketones which are obvious in the appearance of the bands C=O of the carbonyl group in 1715 cm^{-1} (Yagoubi et al., 2015; Antunes et al., 2017; Mandal et al., 2018). Basically, the degradation of polyethylene progresses via a radical chain reaction mechanism is consisting of three common steps, namely, initiation, propagation and termination (Roé-Sosa et al., 2015).

2.3.3(a) Mechanism I (Chain Initiation)

Photocatalyst (eg. TiO_2 , ZnO , etc) has a photocatalytic effect on the degradation of polyethylene (PE) (Castillo-Reyes et al., 2019; Zapata et al., 2019; Kamalian et al., 2018), polypropylene (PP), polyvinyl chloride (PVC) (Fa et al., 2011; Yousif et al., 2019) and polystyrene (PS) (Nakatani et al., 2016). The photodegradation activity of photoexcited photocatalyst (eg. ZnO or TiO_2 , etc) on PE could be achieved through generation of active free hydroxyl radical ($\bullet\text{OH}$) (Jašková et al., 2013). When photocatalyst is bombarded by UV light with energy higher than its bandgap energy (E_g), it creates electrons (e^-) and holes (h^+) pairs (Equation 2.1). Adsorbed oxygen molecules (O_2) and water (H_2O) on the surface can seize e^- and h^+ , producing reactive radicals ($\text{OH}\bullet$, $\text{O}_2^{\bullet-}$, h^+) (Equations (2.2) - (2.8)). Which is very critical reactive radicals for the photodegradation activity. The reduction of oxygen (O_2) would be the vital process in photocatalytic reduction due to the reactions proceed typically with oxygen molecules (O_2) in air.

Oppositely, oxidation of water (H_2O) would be the key process in photocatalytic oxidation when the surface of photocatalysts is shielded with adsorbed

H₂O molecules in common environments. As it can be seen in Figure 2.3, when O₂ is reduced by one electron (Equation 2.2), it becomes a superoxide radical (O₂^{•-}) and reacts with adsorbed water to generate hydrogen peroxide (H₂O₂) (Equation 2.4-Equation 2.6). These reactive radicals (OH[•], 2OH[•]) further strike the neighbouring LDPE polymer chains which produce carbon-centered radicals such as -•CH-CH₂- (Equation 2.9) as shown in Figure 2.4.



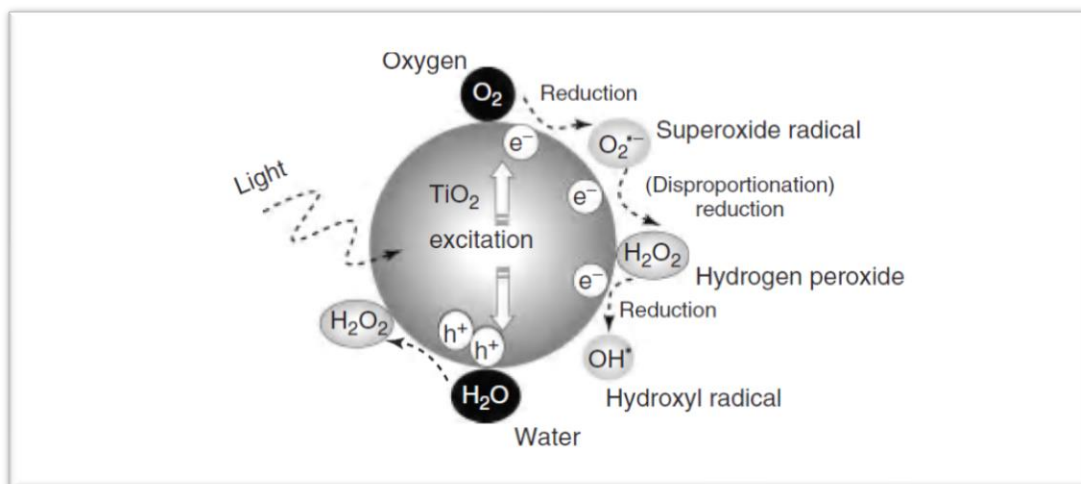


Figure 2.3 One-electron reduction steps of oxygen to OH radical and two-electron oxidation step of water to H₂O₂ observed in the TiO₂ photocatalyst (Nosaka and Nosaka, 2013).

2.3.3(b) Mechanism II (Chain Propagation)

In chain propagation mechanism, the $\cdot\text{CH-CH}_2\cdot$ or alkyl radicals reacts with adsorbed O₂ and form peroxy radicals $\text{-CH}_2\text{-CH-O-O}\cdot$. This peroxy radicals abstract hydrogen from $\text{-CH}_2\text{CH}_2\text{-}$ and lead to form hydroperoxide $\text{-CH}_2\text{-CH-O-OH}$ through hydroperoxide photolysis. And $\text{-CH}_2\text{-CH-O-OH-}$ could receive photon energy to form alkoxy radicals $\text{-CH}_2\text{-CH-O}\cdot$ and hydroxyl radical $\cdot\text{OH}$ or react with $\cdot\text{CH-CH}_2\cdot$ and form $\text{-CH}_2\text{-CO-CH}_2\text{-}$, $\cdot\text{CH-}$ and H₂O (Equations (2.10)-(2.13)).

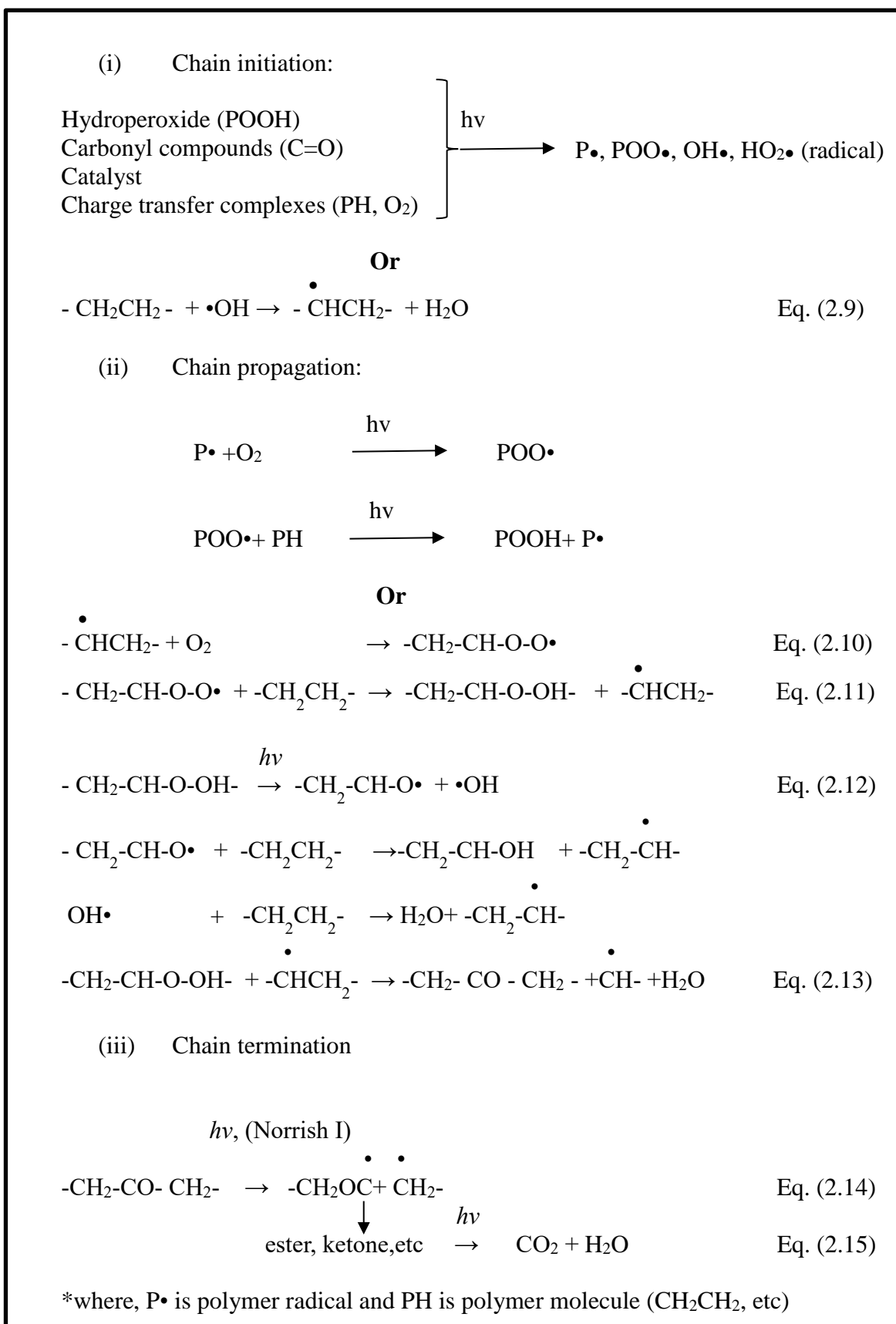


Figure 2.4 Mechanism Photooxidation in Polyethylene (Yousif and Haddad, 2013).

2.3.3(c) Mechanism III (Chain Termination)

Beside the hydroperoxide photolysis in Mechanism II, the second major contributors to the photodegradation of polymers is ketone photolysis in chain termination Mechanism III. The $\text{-CH}_2\text{-CO-CH}_2\text{-}$ in Mechanism II continues through Norrish reaction (mostly with Norrish I with free radical generation and no chain cleavage) (Equation 2.14) and further decompose to carbonyl groups such as aldehyde, ketone, ester, carboxylic acid. Eventually, these carbonyl groups can be further photo-oxidized (receiving photon) to carbon dioxide (CO_2) and water (H_2O) Equation 2.15.

2.4 Factor Affecting the Photocatalyst and Polymer Degradation

Polymer degradation is triggered by several factors discussed in the succeeding sections.

2.4.1 Choice of Photocatalyst

Various photocatalysts have been used to decompose organic pollutant. Among several materials that used as for the photocatalysis are a semiconductor material like TiO_2 , ZnO , CdS , ZnS , ZrO_2 , and MgO . This photocatalyst will produce surface oxidation to eliminate harmful substance such as organic compound (plastic waste or water pollutant or bacteria). It is also called as the photocatalytic detoxification that leads to a complete mineralization where organic compounds are oxidized to CO_2 and H_2O (Figure 2.5).

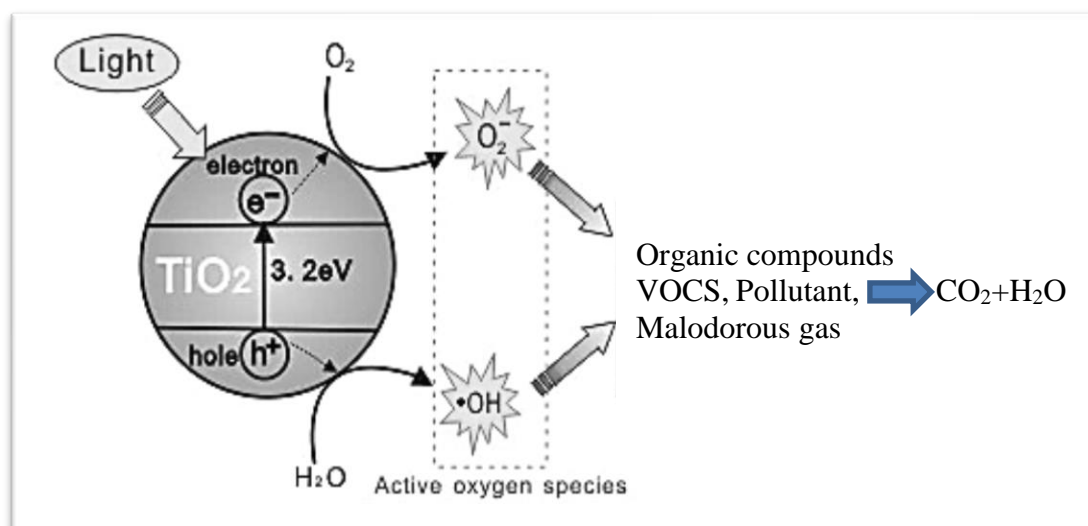


Figure 2.5 Using energy from light, TiO_2 creates two oxidation reactants: hydroxyl radicals ($\cdot\text{OH}$) and superoxide anion ($\text{O}_2^{\cdot-}$) which decomposes toxic organic substance by oxidation (Ibhadon and Fitzpatrick, 2013).

2.4.1(a) Photocatalyst to Degrade Organic Pollutant

Among various photocatalyst, Titania or TiO_2 is extensively used to degrade polymer. TiO_2 is a potential photocatalyst due to its high photoactivity (Li et al., 2015; Yu et al., 2018), non-photocorrosion, low cost (Li et al., 2016b; Humayun et al., 2018), chemical stability (Sharon et al., 2016; Moradi et al., 2016; Li et al., 2017) and low-toxicity (Bhanvase et al., 2017). The band gap (E_g) value of rutile is 3.0 eV, while anatase is 3.2 eV, both can be excited by ultraviolet rays (Li et al., 2016b).

In the last few decades, ZnO has received attention in the degradation of plastic (Lee et al., 2016; Das et al., 2017) as ZnO (3.37 eV) has comparable bandgap as TiO_2 (3.2 eV), thus its photocatalytic ability is expected to equal to that of TiO_2 , due to it has been reported to have higher photocatalytic efficiency when compared to TiO_2 (Qi et al., 2017; Chin Boon et al., 2018) and its capability to absorb a wide range of solar spectrum, more light quanta, due to its direct bandgap and high exciton binding energy